Molecular Biology of the Cell
Vol. 17, 4105–4117, September 2006

Capacity of the Golgi Apparatus for Cargo Transport Prior to Complete Assembly

Shu Jiang,* Sung W. Rhee,* Paul A. Gleeson,† and Brian Storrie*

*Department of Physiology and Biophysics, University of Arkansas for Medical Sciences, Little Rock, AR 72205; and †Department of Biochemistry and Molecular Biology and Bio21 Molecular Science and Biotechnology Institute, The University of Melbourne, Melbourne, Victoria 3010, Australia

Submitted December 7, 2005; Revised June 19, 2006; Accepted July 5, 2006
Monitoring Editor: Vivek Malhotra

In yeast, particular emphasis has been given to endoplasmic reticulum (ER)-derived, cisternal maturation models of Golgi assembly while in mammalian cells more emphasis has been given to golgins as a potentially stable assembly framework. In the case of de novo Golgi formation from the ER after brefeldin A/H89 washout in HeLa cells, we found that scattered, golgin-enriched, structures formed early and contained golgins including giantin, ranging across the entire *cis* to *trans* spectrum of the Golgi apparatus. These structures were incompetent in VSV-G cargo transport. Second, we compared Golgi competence in cargo transport to the kinetics of addition of various glycosyltransferases and glycosidases into nascent, golgin-enriched structures after drug washout. Enzyme accumulation was sequential with *trans* and then medial glycosyltransferases/glycosidases found in the scattered, nascent Golgi. Involvement in cargo transport preceded full accumulation of enzymes or GPP130 into nascent Golgi. Third, during mitosis, we found that the formation of a golgin-positive acceptor compartment in early telophase preceded the accumulation of a Golgi glycosyltransferase in nascent Golgi structures. We conclude that during mammalian Golgi assembly components fit into a dynamic, first-formed, multigolgin-enriched framework that is initially cargo transport incompetent. Resumption of cargo transport precedes full Golgi assembly.

INTRODUCTION

Despite its key importance as the central organelle within the secretory pathway, Golgi apparatus assembly remains poorly understood (for a general review, see Shorter and Warren, 2002). The problem is complex and has been studied in several different systems. In yeast, attention has been drawn repeatedly to the relationship between the Golgi apparatus and the endoplasmic reticulum (ER). In particular, in *Pichia pastoris*, evidence has been presented for the de novo formation of individual Golgi apparatus membrane stacks in association with discrete ER exit sites (Bevis *et al.*, 2002). In *Saccharomyces cerevisiae*, where ER exit is not organized into discrete export zones, evidence has been presented for the ER derivation of Golgi apparatus membranes in the newly formed bud (Reinke *et al.*, 2004). The appearance of a late Golgi marker in the bud was dependent on the appearance of an early Golgi marker, consistent with the expectations of a cisternal progression/maturation model. In mammalian cells, in contrast, more emphasis has been given to the potential role of Golgi membrane clusters and Golgi matrix proteins in organizing Golgi assembly. Golgi matrix proteins belong to the golgin family of coiled-coiled–rich proteins and are often, but not always, e.g., giantin, peripherally associated with Golgi apparatus membranes (for review, see Short *et al.*, 2005). These proteins may serve a structural role in organizing Golgi apparatus membranes and subcompartments and as such may have a membrane organizing role in both mitotic and de novo mammalian Golgi assembly.

In mammalian cells, the long recognized example of Golgi apparatus assembly is mitosis in which the juxatnuclear Golgi apparatus by light microscopy breaks down into scattered fluorescent punctae and mitotic haze and then reassembles (for review, see Shorter and Warren, 2002). The mitotic haze is below the resolving power of the light microscope and its underlying nature has been the subject of debate. On the one hand, evidence has been presented that the mitotic haze is due to reabsorption of Golgi proteins into the ER (Zaal *et al.*, 1999), and on the other hand that the mitotic haze is due to vesicularization of much of the Golgi apparatus into small vesicles (Axelsson and Warren, 2004). The predominance of data today favors vesicularization. ER-specific trapping assays produced no evidence that Golgi proteins accumulate in the ER during mitosis (Pecot and Malhotra, 2004). By confocal fluorescence microscopy, the fluorescent puncta retain subcompartmentalization with *cis*- and *trans*-Golgi markers being resolved in distribution (Shima *et al.*, 1997). Puncta are abundant in some cell examples and rare in others (Puri *et al.*, 2004). The high-resolution technique of electron microscopy reveals the fluorescent puncta to consist of tubular-vesicular membrane clusters (Shima *et al.*, 1997; Jokitalo *et al.*, 2001). A present consensus view is that mitotic clusters never fully breakdown. During the later phases of mitosis, the clusters and mitotic haze come together in a poorly understood process to produce a reassembled Golgi apparatus. Recent evidence suggests mitotic Golgi inheritance is regulated by the modulation of cellular activities that control Golgi protein cycling into and out of the ER (Altan-Bonnet *et al.*, 2006). In the mammalian cell, de novo Golgi apparatus assembly appears to occur in

This article was published online ahead of print in *MBC in Press* (http://www.molbiolcell.org/cgi/doi/10.1091/mbc.E05–12–1112) on July 12, 2006.

Address correspondence to: Brian Storrie (StorrieBrian@uams.edu).

association with ER exit sites during Golgi scattering in response to microtubule depolymerization (Cole *et al.*, 1996; Yang and Storrie, 1998; Storrie *et al.*, 1998) and in response to washout of the drugs brefeldin A and H89 (Puri and Linstedt, 2003). The combined effect of BFA and H89 treatment is to redistribute both Golgi transmembrane proteins and golgins to the ER from which de novo assembly occurs (Puri and Linstedt, 2003). The first detectable step in de novo Golgi assembly is the formation of a post-ER structure positive for the golgin GM130 and cargo receptor gp27 (Puri and Linstedt, 2003; Kasap *et al.*, 2004). This golgin-positive nascent Golgi structure appears to have an acceptor role in subsequent complete Golgi apparatus assembly.

In the present work, we have tested, using a mammalian cell system, when during de novo Golgi assembly the nascent organelle becomes active in cargo transport. Our working hypothesis was that in a staged, golgin-first process that the initial golgin-rich framework would be insufficient for a functional Golgi apparatus in cargo transport. A temperature-sensitive variant of VSV-G protein, tsO45G, was used as the test cargo. We found that early forming structures in Golgi assembly that were rich in a general framework of *cis*- to *trans*-golgins, including giantin, were inactive in cargo transport. The overall kinetics of de novo Golgi assembly was ordered with a sequential accumulation of trans then medial glycosyltransferases/glycosidases in golgin-positive structures. Cargo accumulation in scattered, nascent Golgi structures corresponded with the coaccumulation of medial Golgi enzymes and golgins. Importantly, cargo transport competence preceded full accumulation of enzymes and in particular the protein GPP130 in nascent Golgi. Transport of tsO45G to the cell surface occurred initially from scattered, nascent Golgi structures rather than from a fully formed, juxtanuclear Golgi ribbon. To test whether these detailed kinetics could be relevant to mitotic Golgi assembly, we scored the accumulation of golgins and glycosyltransferases in fluorescent puncta as cells exited mitosis. We found that the formation of a golgin-positive acceptor compartment in early telophase preceded the accumulation of a Golgi glycosyltransferase in nascent Golgi structures. We conclude formation of a golgin-enriched assembly framework and the formation of a cargo transport competent Golgi apparatus constitute separate, but sequentially related stages in Golgi apparatus assembly.

MATERIALS AND METHODS

Cell Culture

Wild-type HeLa cells were grown in DMEM supplemented with 10% fetal bovine serum (FBS) under standard tissue culture conditions. HeLa cells stably expressing tagged Golgi apparatus proteins were maintained in the presence of 0.45 mg/ml G-418 sulfate (Storrie *et al.*, 1998). Cells were grown in a humidified incubator at 37°C and 5% CO_2.

BFA or BFA/H89 Treatments and Washout

HeLa cells were treated with BFA as described previously (Jiang and Storrie, 2005) and with BFA+H89 in a manner similar to that of Puri and Linstedt (2003). To disperse Golgi region proteins, cells cultured on glass coverslips were incubated with 5 μg/ml BFA (Sigma Chemical Company, St. Louis, MO) for 30 min with or without treatment of 100 μM H89 (Sigma) for 10 min at 37°C in the presence of 100 μg/ml cycloheximide (CHX, Sigma). For BFA or BFA+H89 washout, coverslips were transferred between a series of tissue culture dishes and transferred to warmed dishes for a Golgi reformation period at 32 or 15°C.

Nocodazole Treatment

To depolymerize microtubules, after BFA or BFA+H89 washout, GalNAcT2-GFP HeLa cells or wild-type HeLa cells injected with tsO45-VSV-G–encoding plasmids were incubated with 10 μM nocodazole (Sigma) for different period at 32, 39.5, or 15°C.

Microinjection and Incubation of Cells with tsO45-VSV-G–encoding Plasmids

Wild-type HeLa cells were microinjected at room temperature with plasmid encoding tsO45-GFP protein, incubated at 39.5°C either for 6 h or for 5 h and 20 min, followed by BFA or BFA+H89 treatment and washout, and then fixed immediately or shifted to 32 or 15°C. To chase tsO45-VSV-G from the ER to the Golgi apparatus and plasma membrane, cells were incubated in the permissive temperature, 32°C, for 15 and 30 min, and 1, 2, and 3 h. To chase tsO45-VSV-G from the ER to the intermediate compartments, cells were transferred to 15°C for 2 h. Chases were in the presence of CHX.

Live-Cell Imaging

For live-cell microscopy, HeLa cells stably expressing GalNAcT2-GFP were viewed with a Zeiss Axiovert 200M microscope (Carl Zeiss, Thornwood, NY) fitted with a Fluar 40/1.3 numerical aperture (NA) objective, optovar set at 2.5× and a bottom-mounted Roper CoolSNAP HQ CCD camera (Roper Scientific, Photometrics, Tucson, AZ). The camera was operated at 1 × 1 binning. After BFA/H89 washout, cells were maintained on the microscope stage at 32°C in presence or absence of nocodazole. Cells were in a heated chamber (20/20 Technology, Whitehouse Station, NJ) in complete DMEM medium that had been pre-equilibrated in a CO_2 incubator. The chamber was supplied with 5% CO_2 from a mixed air–CO_2 tank.

Antibodies

The following antibodies were used: The clone 35 mouse antibody directed against GM130 was purchased from BD Biosciences (San Diego, CA). Rabbit polyclonal IgG antibodies directed against Sec31a or Sec13a were gifts from Dr. Wanjin Hong (Singapore). Rabbit polyclonal IgG antibodies directed against GCC88 have been described previously (Luke *et al.*, 2003). The mouse mAb directed against GPP130 was a gift from Dr. Adam Linstedt (Carnegie Mellon University, Pittsburgh, PA). Mouse mAb directed against giantin was a gift from Dr. H.-P. Hauri (Biozentrum, University of Basel, Basel, Switzerland). Affinity-purified rabbit and sheep polyclonal IgG antibodies directed against GRASP65 or GRASP55, respectively, were gifts from Dr. Francis Barr (Max Planck Institute for Biochemistry, Martinsried, Germany). Mouse monoclonal antibodies directed against GalT were gifts from Dr T. Nilsson (EMBL, Heidelberg, Germany). 9E10 mouse monoclonal antibodies directed against the myc peptide were prepared by Alan Sawyer (EMBL). Affinity-purified rabbit polyclonal antibodies directed against the VSV-G epitope have been described previously (Röttger *et al.*, 1998). The sheep antibody directed against TGN46 was purchased from Serotec (Oxford, United Kingdom). The mouse mAb directed against human protein disulfide isomerase (PDI) was a gift from Dr. Charlotte Kaetzel (Case-Western Reserve University, Cleveland, OH). Cy3- or Cy5-conjugated donkey anti-mouse, -rabbit, -sheep, or -goat IgG antibodies were obtained from Jackson ImmunoResearch Laboratories (West Grove, PA).

Immunofluorescence Microscopy and Image Analysis

HeLa cells grown on glass coverslips were fixed in 3.5% formaldehyde in PBS for 20 min and permeabilized/blocked with 0.1% saponin/0.2% fish skin gelatin in phosphate-buffered saline (SG/PBS). Cells were incubated for 20 min with primary antibody diluted in SG/PBS. The cells were washed three times with SG/PBS and incubated for 20 min with secondary antibody diluted in SG/PBS. Cells were again washed three times in PBS and mounted on microscope slides in Mowiol. In some experiments, cells were permeabilized in 0.1% Triton X-100 rather than saponin. To identify cells in mitosis in asynchronous cell populations, cells were stained with DAPI. Wide field images were taken using a Zeiss Axiovert 200M microscope with 63/1.4 NA objective, optovar set at 1.6×, and a Roper CoolSNAP HQ CCD camera. The camera was operated at 2 × 2 binning. Spinning-disk confocal image stacks were obtained using a CARV I or II accessory (Atto Bioscience, Rockville, MD; now BD Bioimaging) mounted to the sideport of the Zeiss Axiovert 200M microscope. The 63/1.4 NA objective, optovar set to 1.6×, was used and images were captured to a Retiga EXi camera (QImaging, Burnaby, British Columbia, Canada). The images were processed with Apple Macintosh computers using IPlab 3.9.5 software (Scanalytics, Fairfax, VA) and Adobe Photoshop 7.0 software (San Jose, CA). Gray-scale values were mapped to an optimal intensity range in most cases.

For the analysis of mitotic cells, cells were identified in wide field and confocal images taken at approximately midcell depth were analyzed. Most images were collected randomly with respect to mitotic phase. However, as analysis revealed that Golgi assembly was initiated in early telophase, additional selective micrographs were taken to enrich the data set in cells falling into early telophase. We identified cells in early telophase by dual wavelength imaging: fluorescence for DAPI and phase contrast for general cell shape (see below). For analysis, cells falling into four groups were scored: 1) metaphase: round cells with condensed chromosomes located at the center, 2) anaphase: round cells that show clear separation of chromosomes into two groups, 3) early telophase: rounded cells with indentation of 20–80% of the cell diameter, and 4) late telophase: connected daughter cells without decondensation of chromosomes.

Images were analyzed using IPLab 3.9.5 software for the distribution of GalNAcT2-GFP, GM130, GalT, and GPP130 in bright puncta using intensity and size threshold criteria. For each image, we first measured the intercellular

Table 1. Properties of Golgi marker proteins assessed

Protein	Integral membrane protein	Cisternal location	Endogenous or tagged detected	Reference
Golgins/GRASPs				
GM130	Peripheral	*cis*	Endogenous	Nakamura *et al.* (1995)
GRASP65	Peripheral	*cis*	Endogenous	Barr *et al.* (1997)
Giantin	Yes (Type II)	*cis*	Endogenous	Linstedt and Hauri (1993)
GRASP55	Peripheral	Medial	Endogenous	Shorter *et al.* (1999)
GCC88	Peripheral	TGN	Endogenous	Luke *et al.* (2003)
Glycosyltransferases/Glycosidases				
NAGT-I	Yes (Type II)	Medial	Myc-tagged	Nilsson *et al.* (1993)
GalNAcT2	Yes (Type II)	*cis* to *trans*	GFP-tagged	Storrie *et al.* (1998)
Mann II	Yes (Type II)	Medial	VSV-tagged	Rabouille *et al.* (1995)
SialylT	Yes (Type II)	*trans*/TGN	VSV-tagged	Rabouille *et al.* (1995)
GalT	Yes (Type II)	*trans*/TGN	Endogenous	Nilsson *et al.* (1993)
Misc. nonenzymatic				
GPP130	Yes (Type II)	*cis*	Endogenous	Linstedt *et al.* (1997)
TGN46	Yes (Type I)	TGN	Endogenous	Prescott *et al.* (1997)

background fluorescence intensity (BG). For each cell, the average cytoplasmic fluorescence intensity (CI) outside the visibly identifiable bright spots was determined and a fluorescence intensity threshold was calculated as CI + 1.5 × (CI − BG). The minimum size criterion for bright fluorescent punctae was 20 adjacent pixels (equivalent to 0.1 μm^2 in size). The appropriateness of criteria was verified against visual identification of bright puncta. The IPLab script is available on request.

RESULTS

We chose HeLa cells for these experiments because of the wide array of antigen-detectable and/or well-characterized, tagged Golgi proteins available within this cell line. These include the 12 different Golgi apparatus proteins utilized (3 golgins, 2

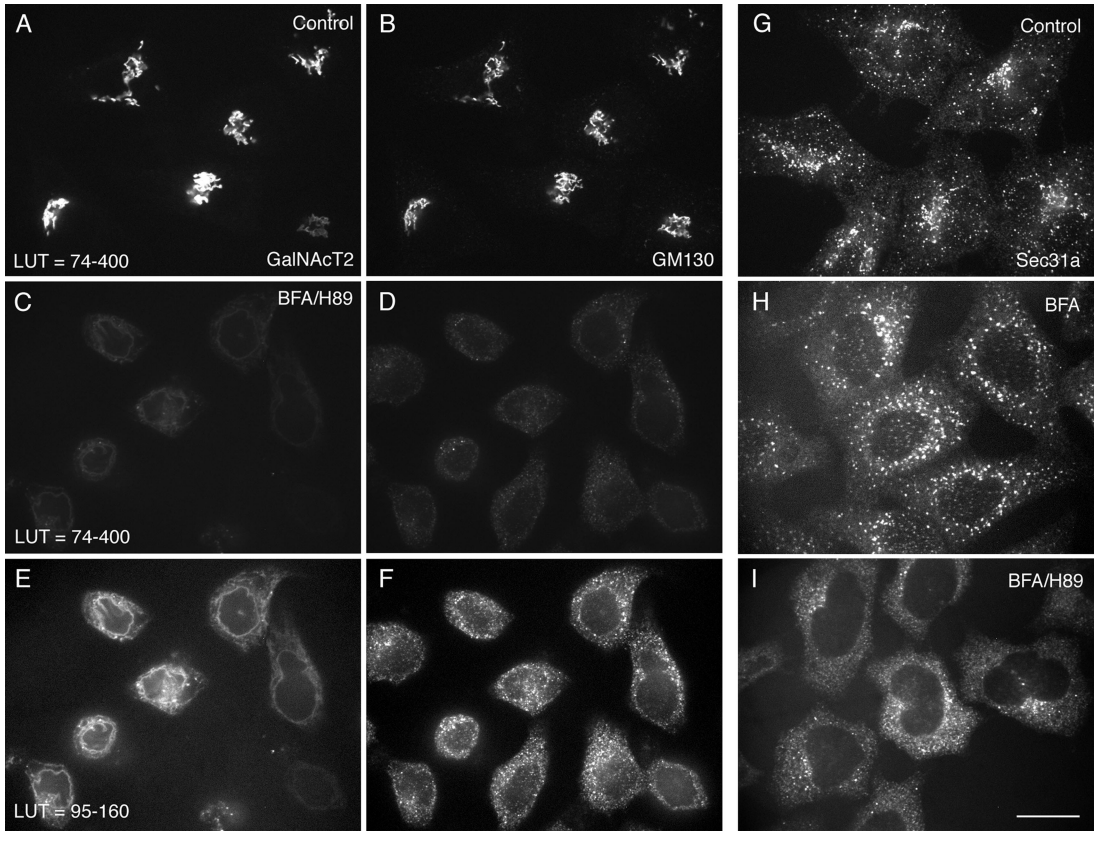

Figure 1. BFA/H89 disperses GalNAcT2-GFP and GM130 into ER-like structures with extensive ER exit site breakdown. HeLa cells stably expressing GalNAcT2-GFP were left untreated (A, B, and G), treated with BFA for 30 min supplemented with H89 for the last 10 min of BFA treatment (C–F and I), or treated with BFA for 30 min at 37°C (H). The localization of GalNAcT2-GFP was determined, and cells were stained for GM130 or Sec31a (ER exit marker) by immunofluorescence. All GalNAcT2 images were taken at the same exposure conditions. Similarly the GM130 images were taken at constant exposure conditions. Images as indicated are displayed to different LUT (lookup table). All micrographs were taken with a CARV I spinning disk confocal device. Bar, 10 μm.

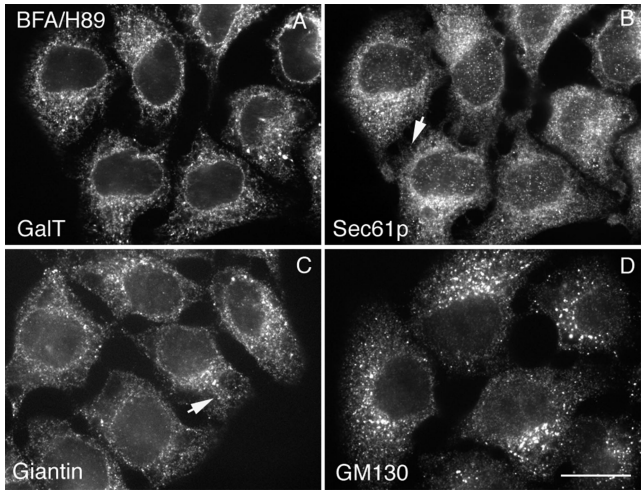

Figure 2. BFA/H89 treatment produces ER localization of Golgi membrane proteins with a more granular redistribution of GM130. Wild-type HeLa cells were treated with BFA supplemented with H89, and then cells were fixed and costained for Sec61p (B) with GalT (A), Giantin (C), or GM130 (D) each individually. GalT and Giantin redistributed to an ER and showed extensive colocalization with Sec61p, whereas GM130 displayed more granular ER-like pattern: beads-on-a-string (arrows). All micrographs were taken with a CARV II spinning disk confocal device. Bar, 10 μm.

GRASPs, 5 glycosyltransferases/glycosidases, and 2 Golgi resident but plasma membrane-cycling proteins). The relevant properties of these proteins are summarized in Table 1. We note that GRASPs are noncoiled-coil, peripheral proteins that interact with golgins and are thought to link Golgi cisternae together (for reviews, see Barr and Short, 2003; Short *et al.*, 2005). In addition, the cargo protein, tsO45G (glycoprotein of the temperature-sensitive Orsay 45 stain of vesicular stomatitis virus), a single-pass, transmembrane protein provided a marker for Golgi apparatus function in secretion.

BFA/H89 Treatment Produces Near-Complete Redistribution of Golgi Apparatus Proteins to the ER

BFA, a fungal metabolite, which blocks activation of the GTPase Arf1, induces redistribution of most Golgi-localized transmembrane proteins to the ER, but Golgi matrix proteins such as GM130 remain associated with so-called Golgi remnants (Nakamura *et al.*, 1995; Seemann *et al.*, 2000). At electron microscope resolution, these consist of tubulovesicular membrane clusters. The protein kinase A inhibitor H89 blocks coat protein II (COPII) recruitment to ER membranes and hence ER export (Aridor and Balch, 2000; Lee and Linstedt, 2000). Puri and Linstedt (2003) reported that combined treatment of cells with BFA alone followed by BFA plus H89 causes ER localization of both matrix and nonmatrix Golgi markers.

We tested by confocal fluorescence microscopy whether combined BFA/H89 treatment of HeLa cells resulted in a complete ER localization of all Golgi proteins. The normal distributions of the Golgi glycosyltransferase, GalNAcT2-GFP, and peripheral golgin, GM130, were both compact and juxtanuclear (nuclei, unpublished data) with extensive correspondence in fluorescence patterns apparent in the micrographs (Figure 1, A and B). In cells exposed to a combined BFA/H89 treatment, the fluorescence intensities for both GalNAcT2 and GM130 were greatly reduced, with both being distributed in a faint pattern encircling the nucleus (Figure 1, C and D). When the lookup table (LUT) by which the images were displayed

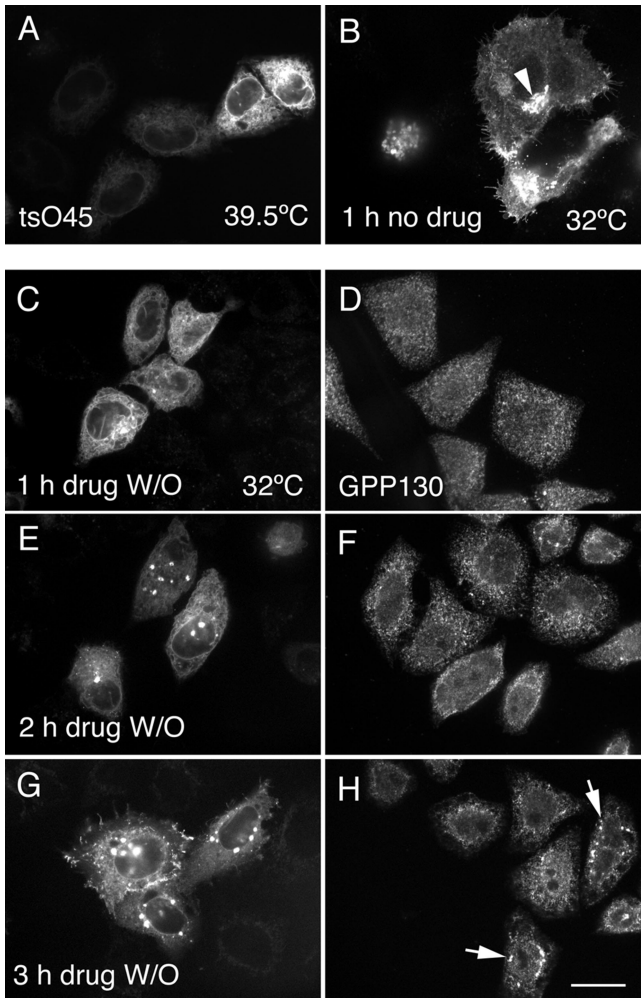

Figure 3. tsO45-VSV-G protein is retained in the ER in the absence of a newly formed Golgi apparatus. Wild-type HeLa cells were microinjected at room temperature with plasmid encoding tsO45G-GFP protein, incubated at 39.5°C for 6 h, and then fixed immediately (A) or shifted to the permissive temperature, 32°C, for 1 h (B) in the presence of 100 μg/ml cycloheximide. In C–E, the cells were incubated at 39.5°C for 5 h and 20 min and then treated with BFA supplemented with H89. BFA/H89 were washed out and the cells were transferred to 32°C for 1 h (C), 2 h (E), or 3 h (G) in the presence of CHX. Parallel cells were stained for GPP130 (D, F, and H). tsO45-G is ER retained in absence of a pre-existing Golgi apparatus. Arrowhead in B points to tsO45G accumulation in juxtanuclear Golgi apparatus. Arrows in H points to GPP130 accumulation in puncta. All micrographs were taken with a CARV II spinning disk confocal device. Bar, 10 μm.

was reset to give more detail, GalNAcT2 was revealed to be distributed in a continuous pattern that rimmed the cell nucleus, whereas the distribution of GM130 appeared more granular (Figure 1, E and F). All further micrographs use LUTs optimized to show detail in the fluorescence distribution. To test whether the combined BFA/H89 treatment had disrupted ER exit sites as expected, separate cells were fixed and stained for the distribution of the COPII coat protein component, Sec31a. As revealed in Figure 1G, Sec31a is normally concentrated in scattered, cytoplasmic puncta and puncta that cluster in the juxtanuclear region in which the Golgi apparatus is concentrated. These punctae can be equated with ER exit sites. With BFA treatment, the scattered, cytoplasmic puncta remain

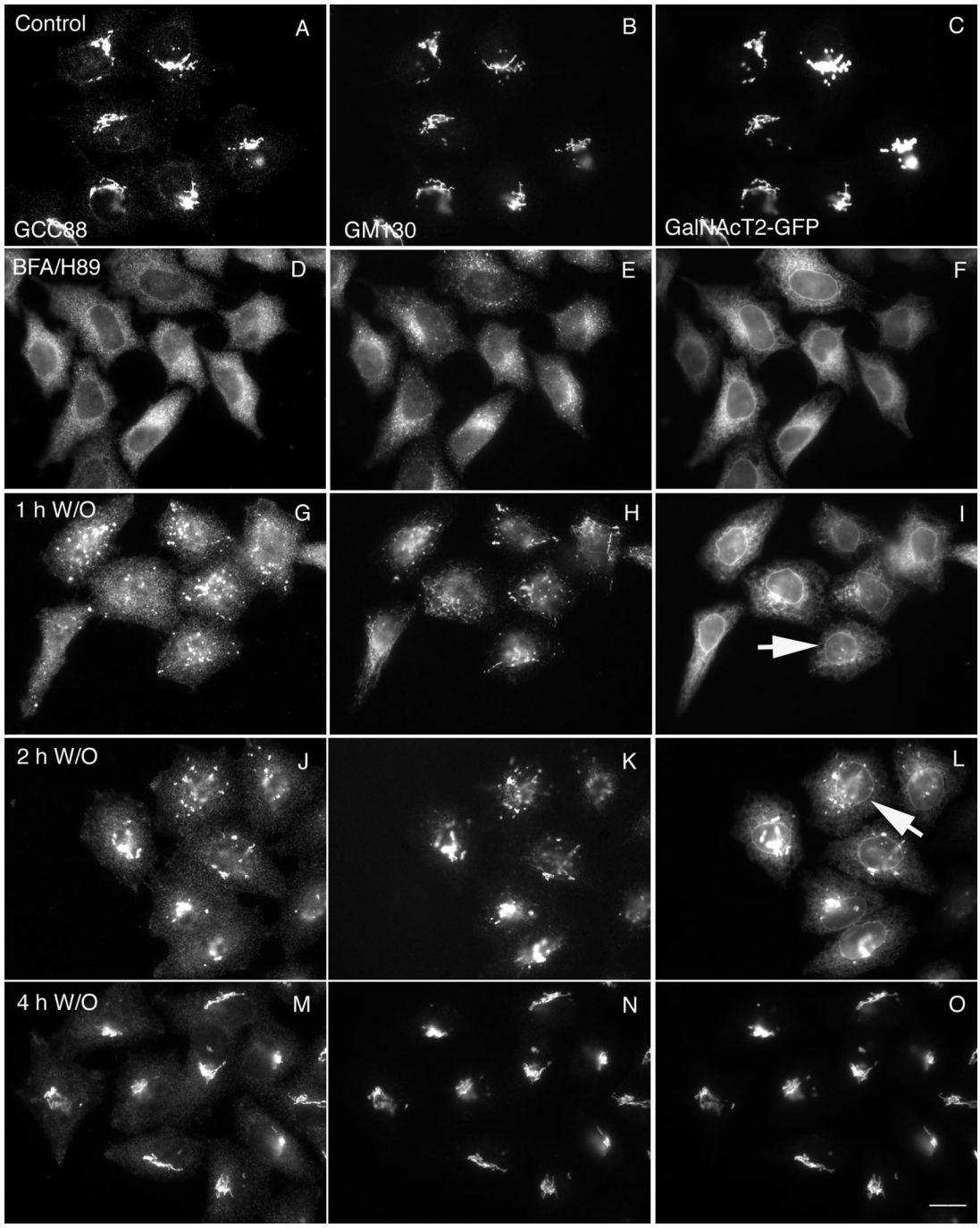

Figure 4. Matrix proteins (GCC88 and GM130) collect into nascent Golgi structures, whereas a glycosyltransferase stays in the ER. HeLa cells stably transfected with GalNAcT2-GFP were double-labeled with GCC88 and GM130 before and after BFA/H89 washout. Each protein was found in a compact juxtanuclear Golgi structure in nontreated cells (A–C). After BFA/H89 washout at 32°C, GCC88 and GM130 displayed similar behavior and accumulated much faster than GalNAcT2 into post-ER punctae (G–L). The juxtanuclear Golgi structure was positive for all after 4 h (M–O). All micrographs were taken with a wide-field Zeiss Axiovert 200M microscope with the camera mounted on the baseport. Arrows in I and L point to examples of nuclear envelope, i.e., ER distribution of GalNAcT2 versus GM130. Bar, 10 μm.

with a loss of the clustered, juxtanuclear puncta (Figure 1H). With BFA/H89 treatment, there was almost complete loss of scattered ER exit sites as indicated by Sec31 staining (Figure 1I). We conclude that the combined treatment was indeed effective in disrupting ER exit sites.

To further characterize the effect of BFA/H89 treatment on the distribution of Golgi proteins, we compared the distribution of a number of Golgi marker proteins to that of two different ER marker proteins, Sec61p (major ER translocon subunit) and protein disulfide isomerase (PDI, an ER luminal protein). As shown in Figure 2, redistributed endogenous β1,4-galactosyltransferase (GalT) and giantin were very similar in distribution to Sec61p or PDI (unpublished data) by confocal fluorescence microscopy. However, there were minor differences in distribution between the proteins. The distributions of GalT and PDI were the most continuous, whereas that of

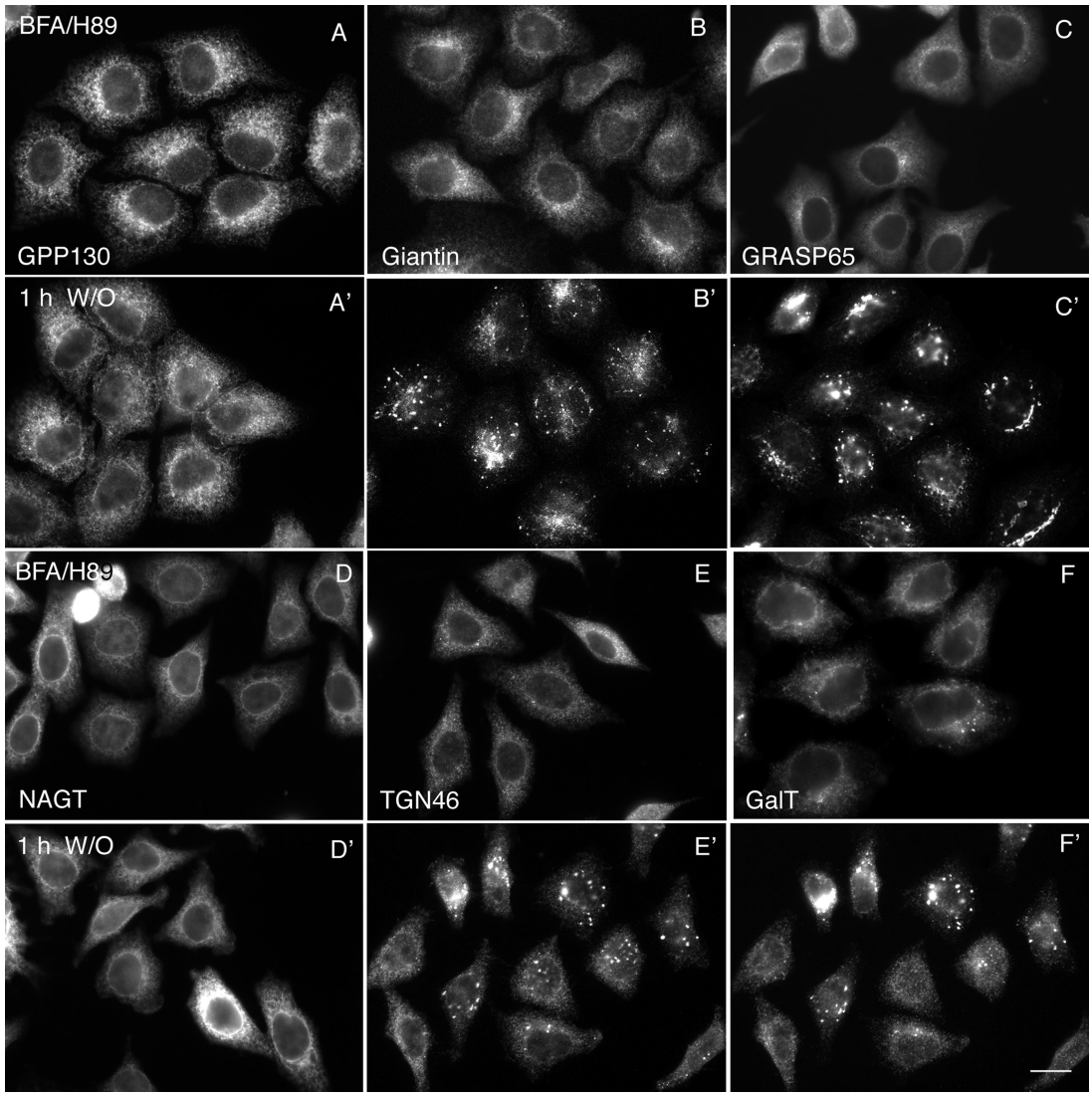

Figure 5. Golgi proteins differ substantially in their kinetics of post-ER accumulation. HeLa cells were treated with BFA/H89 to disperse Golgi proteins (A–F). BFA/H89 were washed out, and the cells were incubated at 32°C for 1 h (A′–F′) in complete culture medium in the presence of 100 μg/ml cycloheximide. Cells were fixed and stained with different antibodies. GPP130 (A), giantin (B), GRASP65 (C), NAGT-I (D), TGN46 (E), and GalT (F) showed ER relocation upon BFA/H89 treatment. After 1-h washout, GRASP65 (*cis* matrix protein) and giantin (*cis* Golgi membrane protein of the golgin family, which complexes with GM130) accumulated in scattered punctuate structures (B′ and C′), and TGN46 and GalT (*trans*-Golgi membrane proteins) exhibited a mixed ER and punctuate structures (E′ and F′). GPP130 (*cis*-Golgi membrane protein) and NAGT-I (medial Golgi membrane protein) remained in the ER (A′ and D′). All micrographs were taken with a wide-field Zeiss Axiovert 200M microscope with the camera mounted on the baseport. Bar, 10 μm.

Sec61p and giantin had a more beads-on-a-string appearance (arrows, Figure 2, B and C). The endogenous GalT immunofluorescence staining was typical of all glycosyltransferases/glycosidases tested. The antibody to endogenous GalT gave bright staining and ER-relocated GalT could be readily detected. The distribution of GM130 was more granular, with little beads-on-a-string appearance. All other tested golgins or GRASPs (e.g., GCC88, see Figure 4A, GRASP65, and Figure 5C, and GRASP55, unpublished data, all wide-field microscopy) gave a disperse distribution in cells treated with BFA or BFA/H89. These proteins may be dispersed into the cytosol as is the peripheral membrane protein COPI with BFA treatment. The distributions of the other six integral Golgi membrane proteins tested were similar to GalT and giantin. We conclude in agreement with Puri and Linstedt that BFA/H89 treatment effectively breaks down Golgi apparatus organization. However, we note the exception of GM130 that in our hands appeared to remain granular in distribution, at least partially, in close association with residual ER exit sites not fully disrupted with H89 treatment. The source of the apparent disagreement between our results for GTM130 and those of Puri and Linstedt (2003) may well be one of how the images are displayed. When mapped to similar LUTs, both we and Puri and Linstedt (2003) find little granularity in the GM130 distribution. Only when the LUT is optimized for the brightness of the distribution does the underlying GM130 granularity become apparent. In our opinion, LUT optimization is appropriate especially considering the ~10-fold dilution in the concentration of Golgi proteins that occurs with redistribution into the ER (Rhee *et al.*, 2005).

We conclude that BFA/H89 treatment is more effective in redistributing Golgi proteins and in disrupting ER exit sites than is treatment of HeLa cells with BFA alone. BFA treat-

Table 2. Kinetics of Golgi proteins accumulation into post-ER structures after BFA/H89 washout at 32°C

		Time after BFA/H89 washout (min)				
Protein		0	30	60	90	120
Golgin/GRASP						
trans	GCC88	ER	Puncta	Puncta	n.d.	Compact
Medial	GRASP55	ER	Puncta	Puncta	Compact	n.d.
cis	GRASP65	ER	Puncta	Puncta	Compact	n.d.
	GMI130	ER[a]	Puncta	Puncta	Compact	Compact
	Giantin	ER	Puncta	n.d.	Compact	n.d.
Golgi membrane protein						
trans	TGN46	ER	ER	ER/Puncta	Puncta	Compact
	GalT	ER	ER	ER/Puncta	Puncta	Compact
	SialylT	ER	ER	ER	ER/Puncta	ER/Puncta
	GalNAcT2-GFP	ER	ER	ER	ER	ER/Puncta
Medial	Mann II	ER	ER	ER	ER	ER/Puncta
	NAGT-I	ER	ER	ER	ER	n.d.
cis	GPP130	ER	ER	ER	ER	ER
Cargo	ts045-VSV-G	ER	ER	ER	n.d.	ER/Puncta

n.d., not determined. For each entry, 40–45 cells were scored visually for the pattern of protein distribution.
[a] The distribution of GM130 after BFA/H89 treatment looks granular.

ment alone does not disrupt most ER exit sites. Furthermore, we conclude that these conditions are effective in redistributing most, albeit, perhaps, not all Golgi matrix proteins into a cytosolic to continuous ER distribution.

Testing Secretory Functionality: Cargo Transport from the ER Depends on Golgi Assembly State

Having confirmed that BFA/H89 treatment produces extensive redistribution of Golgi proteins to the ER, we asked if BFA/H89 washout leads to rapid resumption of secretory trafficking in HeLa cells. Such an outcome is expected based on the rapid, 30-min assembly of Golgi apparatus reported by Puri and Linstedt earlier in 37°C washout experiments. Furthermore, the kinetics of cargo transport from the ER to the plasma membrane are rapid even at 32°C, i.e., ≤1 h. To test for cargo trafficking in the secretory pathway, we probed for tsO45G transport from the ER to the plasma membrane when cells were shifted from 39.5 to 32°C. tsO45G is the temperature-sensitive variant of the spike glycoprotein of vesicular stomatitis virus. At 39.5°C, the protein is synthesized, in our case, tsO45G-GFP, but fails to fold properly and hence accumulates in the ER as shown in Figure 3A. In these experiments, plasmids encoding tsO45G-GFP were microinjected into the cell nucleus. As was apparent from the cell-to-cell variation in fluorescence intensity, there were differences in expression levels. At permissive conditions, 32°C, the protein rapidly folds into its native conformation and normally is exported from the ER to the Golgi apparatus and plasma membrane within 1 h with no need for further protein synthesis, as shown in Figure 3B. The arrowhead in Figure 3B points to the juxtanuclear accumulation of tsO45G in the Golgi apparatus as part of this normal transport process. To our surprise, when HeLa expressing tsO45G protein at 39.5°C were treated with BFA/H89 and then shifted to permissive temperature, drug-free media for 1, 2, or 3 h in the presence of a protein synthesis inhibitor, a considerable delay in tsO45G export from the ER was observed. No export of tsO45G from the ER was detectable by fluorescence at 1 h (Figure 3C). Instead, the distribution of tsO45G-GFP was totally ER-like, with distinct nuclear rim fluorescence and web-like fluorescence throughout the cytoplasm when cells were examined by confocal fluorescence microscopy. For comparison, parallel cells were stained for GPP130, a *cis*-Golgi transmembrane protein, reported by Puri and Linstedt to be delayed in its export from the ER relative to GM130 during BFA/H89 washout at 37°C. As shown in Figure 3D, GPP130 had a slightly granular, ER-like distribution after a 1-h BFA/H89 washout at 32°C, indicating that it like tsO45G was still in the ER. After a 2- or 3-h BFA/H89 washout, a progressive change in the tsO45G distribution was observed. At 2 h, tsO45G had begun to accumulate into post-ER fluorescent patches (Figure 3E) and, by 3 h, there was still some in the ER, as indicated by nuclear rim staining, and in addition tsO45G was present in perinuclear patches and at the cell surface (Figure 3G). Parallel results, albeit slower, were found for GPP130 with respect to its accumulation in perinuclear patches (Figure 3H, arrows point to examples). tsO45G transport results were the same when HeLa cells were treated with BFA alone, a drug treatment that does not disrupt ER exit sites (unpublished data). Moreover, after a 2-h, 15°C BFA/H89 washout, no accumulation of tsO45G in the intermediate compartment/ERGIC was observed, in contrast to the normal pronounced accumulation; instead, the tsO45-G distribution was ER-like (unpublished data). Finally, by wide-field fluorescence microscopy, the golgin, GM130, was found to accumulate in distinct puncta as shown in Figure 4 after a 30-min or 1-h chase at 32°C, whereas tsO45-G remained in the ER (unpublished data).

We raise as an interpretative framework for these experiments the possibility that the assembly state of the Golgi apparatus might feedback upon cargo exit from the ER. Alternatively, different proteins may compete for ER exit more or less efficiently. We note that our acceptor feedback suggestion is supported by the early in vitro experiments of Balch and colleagues (Aridor *et al.*, 1995) in which ER exit is inefficient in the absence of an acceptor compartment.

The Accumulation of Medial Glycosyltransferases/ Glycosidases in Nascent Golgi Structures Is Delayed

We next investigated the assembly state of nascent Golgi structures after a BFA/H89 washout at 32°C. In our approach, we characterized the post-ER accumulation of a number of Golgi apparatus marker proteins summarized in

Table 1. Much of this screening was done by wide-field fluorescence microscopy, 2 × 2 binning, as the quickest approach at giving total cell protein distributions in a single focal plane image. As illustrated in Figure 4, treatment with BFA/H89 resulted in the dispersal of both the *trans*- and *cis*-golgins, GCC88 and GM130, and the Golgi glycosyltransferase, GalNAcT2. Little, if any, of the granularity apparent with GM130 was observed for GCC88 after BFA/89 treatment. After BFA/H89 washout there was progressive accumulation of both GCC88 and GM130 into colabeling punctate structures that displayed a juxtanuclear distribution over time. At short time points such as 15 or 30 min, GCC88 and GM130 had begun to accumulate scattered punctate structures (unpublished data). In contrast, the accumulation of GalNAcT2 into punctate, nascent Golgi structures was delayed, with no obvious accumulations observed after a 1-h washout at 32°C (Figure 4I, arrow points to nuclear rim staining). Even at a 2-h washout where accumulation of GalNAcT2 into punctate structures was obvious, there was still appreciable GalNAcT2 remaining in the ER, as indicated by nuclear rim staining (Figure 4L, arrow). Full Golgi assembly into a compact, juxtanuclear Golgi ribbon was apparent for all three markers by wide-field microscopy at 4 h (Figure 4, M–O). In sum, Golgi assembly is slow at 32°C with both *cis*- and *trans*-golgins accumulating more rapidly into post-ER punctate structures than a Golgi glycosyltransferase. The slow accumulation of GalNAcT2 into post-ER structures is consistent with data trends reported earlier at higher temperatures (Puri and Linstedt, 2003; Kasap *et al.*, 2004). Note: the 2-h accumulation of GalNAcT2 into perinuclear patches was consistent with that observed for tsO45G, albeit GPP130 was slow.

These results suggest that Golgi functionality as an acceptor compartment in the secretory pathway correlates not with the initial assembly of golgin-enriched structures, but rather with the accumulation of glycosyltransferases in these structures. Taking advantage of the abundance of Golgi markers available in HeLa cells, we next asked if cisternal Golgi transmembrane proteins such as NAGT-I, TGN46, and GalT all showed a similar ER export dependence on the Golgi assembly state as did GalNAcT2. As illustrated in Figure 5 and summarized in tabular form in Table 2, the kinetics of ER export, i.e., post-ER accumulation, of Golgi proteins during de novo Golgi reassembly at 32°C, fall into a pattern. All golgins and GRASPs including the *cis*-Golgi transmembrane protein, giantin, and the *cis*-Golgi protein GRASP65 and the medial Golgi protein GRASP55 accumulate with similar, fairly rapid kinetics into scattered punctate structures and then progressively into juxtanuclear Golgi structures by immunofluorescence. It is important to note here the collection of golgin markers and GRASPs includes both peripheral and transmembrane proteins that normally localize to the *cis*-, medial, and *trans*-Golgi apparatus. By spinning disk confocal microscopy, *cis*- and *trans*-golgins were separated, suggesting polarity in their distribution (unpublished data). TGN46, GalT, and SialylT, proteins of the *trans*-Golgi network to *trans*-Golgi apparatus, accumulate more slowly in such structures (see Figure 5 for illustrative examples). This accumulation is followed by the medial Golgi apparatus proteins NAGT-I and mannosidase II and GalNAcT2, found in a *cis*- to *trans*-Golgi apparatus gradient-like distribution normally (see Figure 5 for illustrative examples). Finally, the *cis*-Golgi type I transmembrane protein, GPP130, was slow in its accumulation into post-ER structures. The same kinetic results were found for BFA washout alone, a treatment that does not disturb ER exit sites (unpublished data). Fully reassembled Golgi apparatus supported normal, rapid tsO45 G protein transport from the ER at 32°C (unpublished data).

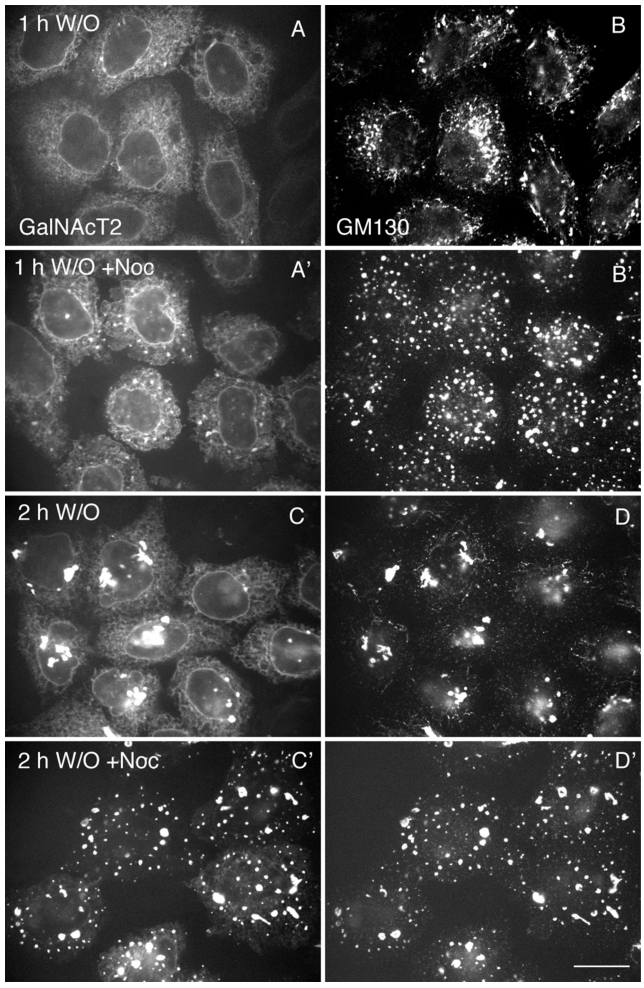

Figure 6. Restriction of nascent Golgi structures to close proximity to ER exit sites accelerates clearance of Golgi components from the ER. HeLa cells stably transfected with GalNAcT2-GFP were treated with BFA/H89. After washout, the cells were incubated at 32°C for 1 or 2 h in the absence (A–D) or presence (A′–D′) of nocodazole (10 μM). The cells were visualized by GFP fluorescence for GalNAcT2-GFP (A, A′, C, and C′) and immunofluorescently stained for GM130 (B, B′, D, and D′). The BFA/H89 washout was in the presence of cycloheximide. All micrographs were taken with a CARV I spinning disk confocal device. Bar, 10 μm.

We conclude from experiments that either 1) the ER exit properties of various Golgi transmembrane proteins must differ greatly with giantin, for example, being very efficient in its export and GalNAcT2 or GPP130 and the cargo protein, tsO45G, being inefficient or 2) the net export, i.e., post-ER accumulation of various proteins, must depend on the downstream acceptor state of the nascent Golgi apparatus. The observation that giantin, a transmembrane golgin, is part of the initial golgin-enriched structures strongly indicates that ER exit sites must be functional early. However, as demonstrated earlier, there is, in essence, no detectable net ER exit of tsO45G protein during the first h of Golgi assembly.

Maintaining Nascent Golgi Structures in Close Proximity to ER Exit Sites Accelerates Golgi Assembly

Numerous observations suggest that de novo Golgi assembly has a close relationship with ER exit sites. In de novo

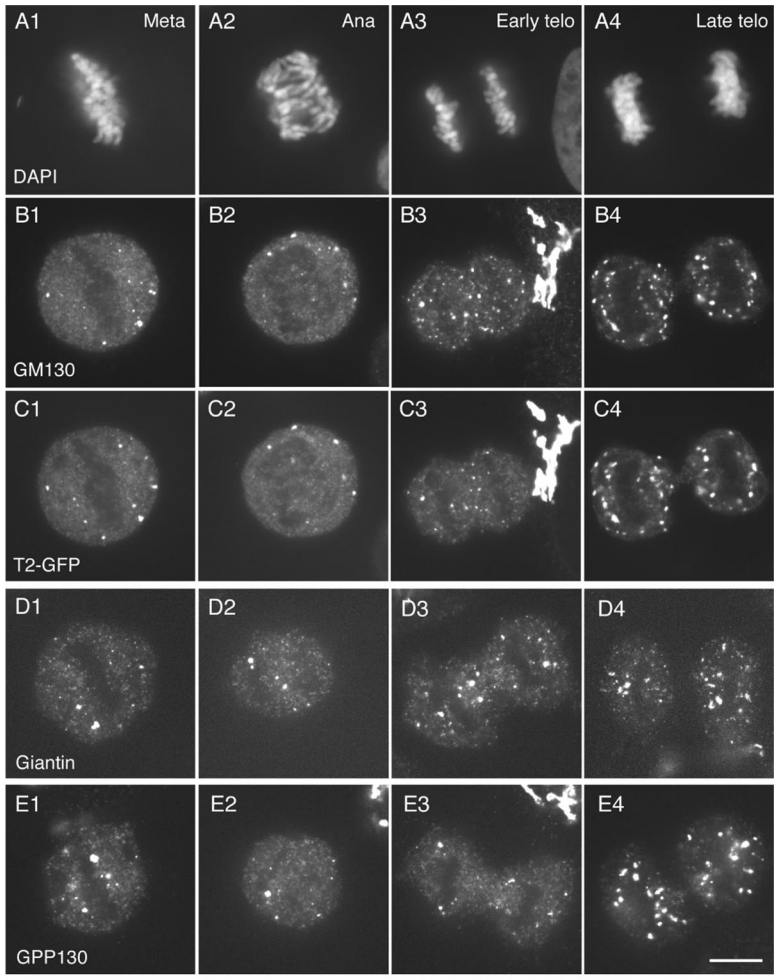

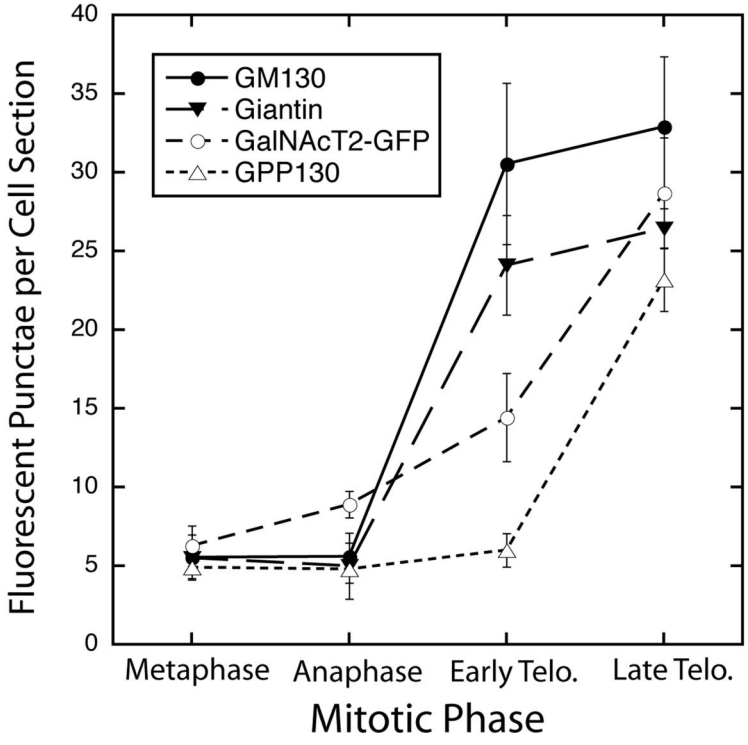

Figure 7. GM130- or giantin-positive nascent Golgi structures accumulate faster than GalNAcT2- or GPP130-positive structures during early telophase. HeLa cells stably transfected for GalNAcT2-GFP were stained with DAPI to visualize chromosomes and GM130 antibody. Wild-type HeLa cells were separately stained with giantin or GPP130 antibodies. Individual cells in the asynchronous population were staged with respect to mitotic phase by appearance of their chromosomes and cell shape in phase-contrast micrographs. All micrographs were taken with a CARV II spinning disk confocal device. The number of cells scored for each data point varied between 9 and 11. (A1–A4) chromosome appearance; DAPI staining. (B1–B4) GM130 distribution; (C1–C4) GalNAcT2-GFP distribution (T2-GFP); (D1–D4) giantin distribution; (E1–E4) GPP130 distribution; (F) quantification of the number of fluorescent punctae versus mitotic phase. Bar, 10 μm.

Golgi assembly at 32°C as shown in Figure 4, there is a progressive perinuclear movement of nascent Golgi structures. We reasoned that this movement might actually slow down Golgi assembly by decreasing the efficiency of downstream capture of newly ER exited vesicles. Capture probability might well be distance dependent. To test this hypothesis, Golgi assembly was monitored by confocal fluorescence microscopy after BFA/H89 washout at 32°C in the absence or presence of nocodazole to depolymerize microtubules. As shown in Figure 6, nocodazole treatment accelerated the accumulation of the glycosyltransferase marker, GalNAcT2-GFP, into nascent Golgi structures. After a 1-h washout, there was accumulation of GalNAcT2 into a subset of the numerous, scattered nascent Golgi structures enriched in GM130. The scattered GM130 structures were in close proximity to ER exit sites, as indicated by Sec31 staining (unpublished data). After a 2-h chase in the presence of nocodazole, there was almost complete clearance of GalNAcT2 from the ER into scattered GM130-positive Golgi assembly elements (Figure 6C′). In contrast, appreciable GalNAcT2 was found in the ER in non–nocodazole-treated cells with some also located in juxtanuclear Golgi foci (Figure 6C). In control experiments, we found that the GalNAcT2- and GM130-positive structures were distinct from ER, as indicated by the lack of any colocalization of staining for the soluble ER protein PDI (unpublished data). By time-lapse fluorescence microscopy, we observed that tracking of nascent, GalNAcT2–GFP-positive, Golgi assembly structures in the presence of nocodazole appeared to be along the ER network (unpublished data). No obvious vesicular intermediates were observed in the presence or absence of nocodazole.

We conclude that maintaining golgin-enriched nascent Golgi assembly structures in close proximity to ER exit sites increases the efficiency of acceptor capture of ER exported proteins. We suggest that net ER exit for individual proteins depends differentially on the progressive development of an acceptor competent Golgi framework.

Golgi Assembly during Mitosis Is Also Seeded by Golgin-positive Structures

Finally, we asked experimentally if there might be any parallels between a golgin-enriched acceptor structure in de novo Golgi assembly and the kinetic phasing of Golgi apparatus assembly at the end of mitosis. To do this, we compared in a quantitative manner the assembly of GM130, giantin, GalNAcT2, and GPP130 into nascent Golgi structures in telophase. Asynchronous GalNAcT2-GFP or wild-type HeLa cell cultures were fixed and stained with DAPI to highlight chromosomes and with GM130, giantin, or GPP130 antibody to highlight the distribution of the individual Golgi protein. Mitotic cells were identified by wide-field fluorescence microscopy and then photographed by spinning disk confocal microscopy at 1×1 binning. Cells were assigned to various portions of mitosis by scoring for chromosome condensation and position versus cell shape and cytokinesis, as indicated by phase contrast microscopy. Experiments were facilitated by the ability to switch rapidly between wide-field and spinning disk confocal microscopy and fluorescence and phase-contrast optics in an integrated optical system.

As shown both qualitatively and quantitatively in Figure 7, there was extensive breakdown of the Golgi apparatus into a few fluorescence puncta, typically, but not always positive for multiple markers and mitotic haze, followed by Golgi reassembly. The extensive breakdown in metaphase is a common observation for HeLa cells (see Puri *et al.*, 2004). We quantified by computer analysis the number of fluorescent puncta $\geq 0.1\ \mu m^2$ per midcell depth section in randomly photographed cells. For metaphase cells, there were ~6 such puncta. During anaphase, there was little change. However, in early telophase, the number increased several-fold for GM130 and giantin but only slightly for GalNAcT2 and GPP130. All GalNAcT2 puncta were positive for GM130. In late telophase, ~25 fluorescent puncta were scored per mid-depth cell section for all four Golgi markers. In late telophase, the chromosomes remain condensed, and there is significant contraction of cytoplasm between the two daughter cells. In sum, the kinetics of Golgi reassembly in mitosis suggests a phased process in which a golgin-enriched structure serves as acceptor for the emergence of glycosyltransferases from the mitotic haze. There does seem to be an apparent similarity with de novo Golgi assembly as observed above.

DISCUSSION

We used a kinetic approach to test the relationship between the formation of golgin-enriched nascent Golgi structures and cargo transport in mammalian cells. Using brief BFA and H89 treatment to disperse Golgi proteins into the ER, we found all three golgins and two GRASPs tested appeared with similar kinetics in rapidly formed, post-ER nascent Golgi structures. The tested golgins and GRASPs included proteins normally located in the *cis*-, medial-, or *trans*-Golgi apparatus and both integral and peripheral membrane proteins. With slower kinetics, the various assayed Golgi glycosyltransferases and glycosidases accumulated in nascent Golgi structures with *trans*-Golgi proteins appearing before medial Golgi enzymes. Functionality in cargo transport as indicated by tsO45G accumulation correlated with the incorporation into nascent Golgi structures of medial Golgi enzymes, in particular. Functionality in cargo transport preceded both the full accumulation of Golgi enzymes and the assembly of a juxtanuclear Golgi ribbon. During mitosis, specifically early telophase, the formation of golgin-positive structures from the mitotic haze preceded the accumulation of a Golgi glycosyltransferase or the *cis*-Golgi protein GPP130 in these structures. We consider the possibility that net export of cargo from the ER is dependent on the acceptor, i.e., assembly state, of the nascent Golgi apparatus and contrast this with the possibility of differential efficiency of protein export from the ER.

Research on Golgi assembly has focused on two different situations. On the one hand, de novo assembly of the Golgi apparatus from the ER has been a significant research thread (for reviews, see Glick, 2002; Puthenveedu and Linstedt, 2005). A major impetus for this line of research has been the popularity in recent years of cisternal maturation/progression models of Golgi function in cargo transport. In such models, new Golgi cisternae form continuously by the fusion of ER-derived carriers. By extrapolation, de novo Golgi formation from the ER is predicted. Experimental evidence for de novo Golgi formation from the ER comes both from work in the yeast *P. pastoris* (Bevis *et al.*, 2002) and *S. cerevisiae* (Reinke *et al.*, 2004) and with mammalian cells (Puri and Linstedt, 2003; Kasap *et al.*, 2004). Much of the mammalian cell work has examined Golgi formation either at scattered sites during microtubule depolymerization or after washout of the drugs BFA or BFA+H89, treatments that disperse Golgi proteins to the ER (Lippincott-Schwartz *et al.*, 1989; Puri and Linstedt, 2003). On the other hand, how the Golgi apparatus is duplicated/sorted/assembled during mitosis has received intense interest over the last 20 years (for review, see Shorter and Warren, 2002). Whether the princi-

ples involved have a common basis across organisms is an open question. In plants, the Golgi apparatus consists of many, scattered individual stacks of Golgi cisternae (for review, see Hawes and Satiat-Jeunemaitre, 2005). Similarly, in *Pichia* (Rossanese *et al.,* 1999), the individual Golgi stacks are isolated from one another. In contrast, in *Saccharomyces*, the Golgi cisternae are not stacked (Rossanese *et al.,* 1999). In mammals, the Golgi apparatus in commonly studied cell types is organized into a juxtanuclear Golgi ribbon that connects together Golgi membrane stacks into a large essentially single organelle (for review, see Shorter and Warren, 2002). This ribbon disassembles during mitosis into scattered tubulovesicular clusters and a mitotic haze. The extent of disassembly into a mitotic haze appears to vary from cell line to cell line. In HeLa cells, few mitotic clusters are observed during metaphase (Puri *et al.,* 2004; present work); much of the Golgi apparatus has broken down into a mitotic haze. Controversy exists with respect to the underlying structural nature of the mitotic haze with the prevailing evidence indicating that the mitotic haze consists of small vesicles (Axelsson and Warren, 2004). Highly controversial evidence has been presented that in mammalian cells Golgi proteins are absorbed into the ER during mitosis and then reemerge at the end of mitosis (Zaal *et al.,* 1999). Recent evidence indicates that cellular activities that control Golgi protein cycling into and out of the ER are important to mitotic Golgi inheritance (Altan-Bonnet *et al.,* 2006).

Our work suggests underlying similarities between de novo, ER-derived Golgi assembly and mitotic Golgi assembly. In both cases, we find that golgin-enriched structures are the prominent early intermediate in Golgi assembly. Golgin-enriched structures may constitute a framework for Golgi assembly. De novo formed golgin structures were positive for all three members of the golgin class of proteins including golgins normally localized to the *cis*-, medial, and *trans*-Golgi apparatus and both peripheral and integral membrane golgins as well as for the two members of the GRASP family tested. Polarity in distribution was apparent in the structures. By spinning disk confocal microscopy, *cis*- and *trans*-golgins were separated. As such, they may provide a general framework into which *trans*-, medial, and *cis* integral membrane proteins such as the Golgi glycosyltransferases and glycosidases are later added. Our results show that the kinetics of addition of these components was sequential at 32°C, the permissive temperature for the transport of presynthesized tsO45-G protein from the ER to the Golgi apparatus. At this temperature, *trans*-Golgi enzymes such as SialylT and GalT accumulated in nascent Golgi structures before medial enzymes such as Mann II or NAGT-I or the *cis*-Golgi integral membrane protein GPP130. A similar order was observed at 37°C. Recent results suggest that COPI coat protein–dependent retrieval mechanisms are unlikely to play an important role in achieving polarity within the Golgi cisternal stack (Bannykh *et al.,* 2005). Our results indicate that a polarized framework is present early during Golgi apparatus assembly. Many of the proteins that we tested are nonessential for secretion, e.g., glycosyltransferases. However, irrespective of this fact, their ordered accumulation in nascent Golgi apparatus must indicate an important underlying feature of Golgi assembly.

On the basis of cell culture experiments, Warren and colleagues (Seemann *et al.,* 2000, 2002) have proposed that a Golgi matrix forms a stable structure that nucleates the de novo and mitotic assembly of the Golgi apparatus. In interphase cells, they find with BFA treatment the presence of Golgi remnants and, with a GTP-restricted ER exit block, they find that, although Golgi enzymes redistribute to the ER, the distribution of the classic marker, the golgin GM130, remains juxtanuclear. In mitotic cells, they find that a matrix marker such as GM130 redistributes during cell division, as predicted for the whole organelle in the presence of either BFA or a GTP-restricted ER exit block. Although the concept of a golgin organized Golgi matrix structures as a nucleation center for Golgi assembly may well have considerable merit, the experiment basis for this proposed by Warren and colleagues has eroded from a number of approaches. Puri and Linstedt (2003) find that combined treatment of cultured cells with BFA and the protein kinase inhibitor H89 disperses golgins and in particular disperses the *cis*-golgin GM130 to the ER (Note: this observation is only partially supported in the present study). In fact, Howell and colleagues (Mardones *et al.,* 2006) find in time-lapse studies that GM130 precedes Golgi enzymes in its appearance in the ER with BFA treatment. Storrie and colleagues (Miles *et al.,* 2001) find that the distribution of golgins is sensitive to an ER exit block when higher concentrations of GTP-restricted Sar1p are used. Moreover, both Lippincott-Schwartz and colleagues (Ward *et al.,* 2001) and Storrie and colleagues (Stroud *et al.,* 2003) find that when GDP-restricted Sar1p is used to block ER exit, a condition that disrupts COPII stabilization of ER exit sites, that there is little, to no, difference in the response of Golgi matrix markers and Golgi enzymes. Both redistribute. Furthermore in cells such as HeLa, there is near complete breakdown of the golgin-rich matrix during mitosis (Puri *et al.,* 2004; present study). Hence, in reality, the previous evidence of stable golgin-rich, Golgi matrix seeding Golgi assembly may well be insubstantial.

We propose, instead, the concept of a dynamic golgin- and GRASP-enriched framework that nucleates Golgi assembly in mammalian cells. In mitotic cells, the assembly of GM130-positive structures during telophase preceded the accumulation in these structures of a Golgi glycosyltransferase or GPP130. In our BFA/H89 washout experiments, the first post-ER assembly intermediate detected by immunofluorescence was a structure positive for a range of golgins and GRASPs. This included the transmembrane proteins giantin. Similarly, Puri and Linstedt (2003) find that GM130 accumulates early in post-ER structures. In previous work, we have shown that a member of the p24 family of transmembrane proteins is an early component of such structures (Kasap *et al.,* 2004). We found in our experiments no evidence for a bolus of Golgi proteins and lipids emerging as a group from the ER. We treated briefly with BFA or BFA+H89 in order to disperse Golgi proteins and lipids into the ER. Recent work indicates that with longer BFA treatment there is a sorting of Golgi proteins and lipids into an ER exit site proximal structure referred to as vesicular tubular cluster or VTC by some (Bannykh *et al.,* 2005; Marondes *et al.,* 2006). The identification of the VTC is supported by electron microscopy. With BFA washout, Bannykh and colleagues find that COPI-independent protein sorting within the VTC gives raise to a polarized stack of Golgi membranes. The role of COPI in establishing Golgi polarity in a golgin-framework seeded assembly situation is for now unknown.

Importantly, our results suggest that the Golgi apparatus becomes functional in cargo transport before assembly of all Golgi components. Interestingly, the post-ER accumulation of golgins including the transmembrane protein giantin and the transmembrane proteins TGN46 or GalT into nascent Golgi structures did not give a Golgi apparatus competent in cargo accumulation; tsO45G remained in the ER. Scattered, nascent Golgi were functional in the post-ER accumulation of cargo before the full clearance of mannosidase II or GalNAcT2 from the ER. Substantial mannosidase II and

GalNAcT2 remained in the ER when tsO45 G accumulation in nascent Golgi structures had begun. Almost all GPP130 was still present in ER. Rather than suggesting a requirement for full Golgi assembly before the resumption of Golgi functionality in cargo transport, our results suggest that scattered nascent Golgi structures containing less than the full amount of Golgi proteins are sufficient. The Golgi marker accumulation kinetics that we observe in telophase suggests that there may well be parallels between de novo Golgi assembly/function and the Golgi apparatus in mitosis. Our data on the interrelationship between Golgi assembly state and cargo transport competency may help to explain the lag between Golgi scattering during microtubule disruption and the ability of these structures to support cargo transport (Cole *et al.*, 1996). Component accumulation in nocodazole scattered Golgi elements is known to be slow for medial versus *trans* enzymes (Yang and Storrie, 1998). In mitosis, Warren and colleagues (Souter *et al.*, 1993) find that transport of HLA as a cargo marker to the Golgi apparatus requires morphological assembly of the organelle only into short, somewhat incomplete appearing, cisternal stacks. How these relate to the presence of a range of Golgi proteins and the relative distribution of these proteins between short cisternal stacks and mitotic "haze" is for now unknown.

Moreover, our experiments suggest that in vivo there is a close functional relationship between ER exit and the organizational state of downstream acceptor compartments in the secretory pathway. We find that if nascent Golgi assembly elements are held near ER exit sites by depolymerizing microtubules that the clearance of Golgi proteins from the ER and presumably the assembly of the Golgi apparatus itself are speeded. We suggest that this experimental outcome is most easily interpreted within a framework in which the assembly state of the downstream acceptor compartment feeds back on ER export. This suggestion regarding a functional relationship between ER exit and the organizational state of the downstream acceptor compartment(s) is fully consistent with the earlier permeabilized cell experiments of Balch and colleagues (Aridor *et al.*, 1995). Alternatively, we suggest that within the framework of differential protein competition for ER exit that the nocodazole outcome could be explained by the hypothesis that holding Golgi assembly elements near to ER exit sites speeds machinery recycling back to the ER.

In summary, we propose a model of Golgi assembly in which a dynamic framework enriched in golgins and some transmembrane proteins but relatively deficient in Golgi glycosyltransferases and glycosidases is the first stage in both de novo and mitotic Golgi assembly. In this model, cargo transport, defining Golgi functionality, resumes before the scattered, nascent organelle units have accumulated their full content of resident proteins. The principles illustrated in this work are directly relevant to the minimum requirements for the assembly of a functional organelle within the secretory pathway. Our conclusions are novel and only possible because of the central experimental approach taken in the present study, the kinetic scoring by fluorescence microscopy of the accumulation of multiple Golgi proteins, 12, in the same cell system.

ACKNOWLEDGMENTS

We gratefully acknowledge the expert technical assistance of Terry Fletcher and Demond Williams. We express our appreciation for gifts of antibodies as cited in *Materials and Methods.* This work was supported in part by grants from the National Science Foundation (MCB-9983332 and MCB-0549001).

REFERENCES

Altan-Bonnet, N., Sougrat, R., Liu, W., Snapp, E. L., Ward, T., and Lippincott-Schwartz, J. (2006). Golgi inheritance in mammalian cells is mediated through endoplasmic reticulum export activities. Mol. Biol. Cell *17*, 990–1005.

Aridor, M., and Balch, W. E. (2000). Kinase signaling initiates coat complex II (COPII) recruitment and export from the mammalian endoplasmic reticulum. J. Biol. Chem. *275*, 35673–35676.

Aridor, M., Bannykh, S. I., Rowe, T., and Balch, W. E. (1995). Sequential coupling between COPII and COPI vesicle coats in endoplasmic reticulum to Golgi transport. J. Cell Biol. *131*, 875–893.

Axelsson, M. A., and Warren, G. (2004). Rapid, endoplasmic reticulum-independent diffusion of the mitotic Golgi haze. Mol. Biol. Cell *15*, 1843–1852.

Bannykh, S. I., Plutner, H., Matteson, J., and Balch, W. E. (2005). The role of ARF1 and rab GTPases in polarization of the Golgi stack. Traffic *6*, 803–819.

Barr, F. A., and Short, B. (2003). Golgins in the structure and dynamics of the Golgi apparatus. Curr. Opin. Cell Biol. *15*, 405–413.

Barr, F. A., Puype, M., Vandekerckhove, J., and Warren, G. (1997). GRASP65, a protein involved in the stacking of Golgi cisternae. Cell *91*, 253–262.

Bevis, B. J., Hammond, A. T., Reinke, C. A., and Glick, B. S. (2002). De novo formation of transitional ER sites and Golgi structures in *Pichia pastoris*. Nat. Cell Biol. *4*, 750–756.

Cole, N. B., Sciaky, N., Marotta, A., Song, J., and Lippincott-Schwartz, J. (1996). Golgi dispersal during microtubule disruption: regeneration of Golgi stacks at peripheral endoplasmic reticulum exit sites. Mol. Biol. Cell *7*, 631–650.

Glick, B. S. (2002). Can the Golgi form de novo? Nat. Rev. Mol. Cell Biol. *3*, 615–619.

Hawes, C., and Satiat-Jeunemaitre, B. (2005). The plant Golgi apparatus—going with the flow. Biochim. Biophys. Acta *1744*, 466–480.

Jiang, S., and Storrie, B. (2005). Cisternal rab proteins regulate Golgi apparatus redistribution in response to hypotonic stress. Mol. Biol. Cell *16*, 2586–2596.

Jokitalo, E., Cabrera-Poch, N., Warren, G., and Shima, D. T. (2001). Golgi clusters and vesicles mediate mitotic inheritance independently of the endoplasmic reticulum. J. Cell Biol. *154*, 317–330.

Kasap, M., Thomas, S., Danaher, E., Holton, V., Jiang, S., and Storrie, B. (2004). Dynamic nucleation of Golgi apparatus assembly from the endoplasmic reticulum in interphase HeLa cells. Traffic *5*, 595–605.

Lee, T. H., and Linstedt, A. D. (2000). Potential role for protein kinases in regulation of bidirectional endoplasmic reticulum-to-Golgi transport revealed by protein kinase inhibitor H89. Mol. Biol. Cell *11*, 2577–2590.

Linstedt, A. D., and Hauri, H. P. (1993). Giantin, a novel conserved Golgi membrane protein containing a cytoplasmic domain of at least 350 kDa. Mol. Biol. Cell *4*, 679–693.

Linstedt, A. D., Mehta, A., Suhan, J., Reggio, H., and Hauri, H. P. (1997). Sequence and overexpression of GPP130/GIMPc: evidence for saturable pH-sensitive targeting of a type II early Golgi membrane protein. Mol. Biol. Cell *8*, 1073–1087.

Lippincott-Schwartz, J., Yuan, L. C., Bonifacino, J. S., and Klausner, R. D. (1989). Rapid redistribution of Golgi proteins into the ER in cells treated with brefeldin A: evidence for membrane cycling from Golgi to ER. Cell *56*, 801–813.

Luke, M. R., Kjer-Nielsen, L., Brown, D. L., Stow, J. L., and Gleeson, P. A. (2003). GRIP domain-mediated targeting of two new coiled-coil proteins, GCC88 and GCC185, to subcompartments of the trans-Golgi network. J. Biol. Chem. *278*, 4216–4226.

Mardones, G. A., Snyder, C. M., and Howell, K. E. (2006). cis-Golgi matrix proteins move directly to ER exit sites by association with tubules. Mol. Biol. Cell *17*, 525–538.

Miles, S., McManus, H., Forsten, K. E., and Storrie, B. (2001). Evidence that the entire Golgi apparatus cycles in interphase HeLa cells: sensitivity of Golgi matrix proteins to an ER exit block. J. Cell Biol. *155*, 543–555.

Nakamura, N., Rabouille, C., Watson, R., Nilsson, T., Hui, N., Slusarewicz, P., Kreis, T. E., and Warren, G. (1995). Characterization of a cis-Golgi matrix protein, GM130. J. Cell Biol. *131*, 1715–1726.

Nilsson, T., Pypaert, M., Hoe, M. H., Slusarewicz, P., Berger, E. G., and Warren, G. (1993). Overlapping distribution of two glycosyltransferases in the Golgi apparatus of HeLa cells. J. Cell Biol. *120*, 5–13.

Pecot, M. Y., and Malhotra, V. (2004). Golgi membranes remain segregated from the endoplasmic reticulum during mitosis in mammalian cells. Cell *116*, 99–107.

Prescott, A. R., Lucocq, J. M., James, J., Lister, J. M., and Ponnambalam, S. (1997). Distinct compartmentalization of TGN46 and beta 1,4-galactosyltransferase in HeLa cells. Eur. J. Cell Biol. *72*, 238–246.

Puri, S., and Linstedt, A. D. (2003). Capacity of the golgi apparatus for biogenesis from the endoplasmic reticulum. Mol. Biol. Cell *14*, 5011–5018.

Puri, S., Telfer, H., Velliste, M., Murphy, R. F., and Linstedt, A. D. (2004). Dispersal of Golgi matrix proteins during mitotic Golgi disassembly. J. Cell Sci. *117*, 451–456.

Puthenveedu, M. A., and Linstedt, A. D. (2005). Subcompartmentalizing the Golgi apparatus. Curr. Opin. Cell Biol. *17*, 369–375.

Rabouille, C., Hui, N., Hunte, F., Kieckbusch, R., Berger, E. G., Warren, G., and Nilsson, T. (1995). Mapping the distribution of Golgi enzymes involved in the construction of complex oligosaccharides. J. Cell Sci. *108*, 1617–1627.

Reinke, C. A., Kozik, P., and Glick, B. S. (2004). Golgi inheritance in small buds of *Saccharomyces cerevisiae* is linked to endoplasmic reticulum inheritance. Proc. Natl. Acad. Sci. USA *101*, 18018–18023.

Rhee, S. W., Starr, T., Forsten-Williams, K., and Storrie, B. (2005). The steady-state distribution of glycosyltransferases between the Golgi apparatus and the endoplasmic reticulum is approximately *90*, 10. Traffic *6*, 978–990.

Rossanese, O. W., Soderholm, J., Bevis, B. J., Sears, I. B., O'Connor, J., Williamson, E. K., and Glick, B. S. (1999). Golgi structure correlates with transitional endoplasmic reticulum organization in *Pichia pastoris* and *Saccharomyces cerevisiae*. J. Cell Biol. *145*, 69–81.

Röttger, S., White, J., Wandall, H. H., Olivo, J. C., Stark, A., Bennett, E. P., Whitehouse, C., Berger, E. G., Clausen, H., and Nilsson, T. (1998). Localization of three human polypeptide GalNAc-transferases in HeLa cells suggests initiation of O-linked glycosylation throughout the Golgi apparatus. J. Cell Sci. *111*, 45–60.

Seemann, J., Jokitalo, E., Pypaert, M., and Warren, G. (2000). Matrix proteins can generate the higher order architecture of the Golgi apparatus. Nature *407*, 1022–1026.

Seemann, J., Pypaert, M., Taguchi, T., Malsam, J., and Warren, G. (2002). Partitioning of the matrix fraction of the Golgi apparatus during mitosis in animal cells. Science *295*, 848–851.

Shima, D. T., Haldar, K., Pepperkok, R., Watson, R., and Warren, G. (1997). Partitioning of the Golgi apparatus during mitosis in living HeLa cells. J. Cell Biol. *137*, 1211–1228.

Short, B., Haas, A., and Barr, F. A. (2005). Golgins and GTPases, giving identity and structure to the Golgi apparatus. Biochim. Biophys. Acta *1744*, 383–395.

Shorter, J., and Warren, G. (2002). Golgi architecture and inheritance. Annu. Rev. Cell Dev. Biol. *18*, 379–420.

Shorter, J., Watson, R., Giannakou, M. E., Clarke, M., Warren, G., and Barr, F. A. (1999). GRASP55, a second mammalian GRASP protein involved in the stacking of Golgi cisternae in a cell-free system. EMBO J. *18*, 4949–4960.

Souter, E., Pypaert, M., and Warren, G. (1993). The Golgi stack reassembles during telophase before arrival of proteins transported from the endoplasmic reticulum. J. Cell Biol. *122*, 533–540.

Storrie, B., White, J., Rottger, S., Stelzer, E. H., Suganuma, T., and Nilsson, T. (1998). Recycling of golgi-resident glycosyltransferases through the ER reveals a novel pathway and provides an explanation for nocodazole-induced Golgi scattering. J. Cell Biol. *143*, 1505–1521.

Stroud, W. J., Jiang, S., Jack, G., and Storrie, B. (2003). Persistence of Golgi matrix distribution exhibits the same dependence on Sar1p activity as a Golgi glycosyltransferase. Traffic *4*, 631–641.

Ward, T. H., Polishchuk, R. S., Caplan, S., Hirschberg, K., and Lippincott-Schwartz, J. (2001). Maintenance of Golgi structure and function depends on the integrity of ER export. J. Cell Biol. *155*, 557–570.

Yang, W., and Storrie, B. (1998). Scattered Golgi elements during microtubule disruption are initially enriched in *trans* Golgi proteins. Mol. Biol. Cell *9*, 191–207.

Zaal, K. J., *et al*. (1999). Golgi membranes are absorbed into and reemerge from the ER during mitosis. Cell *99*, 589–601.